CHEMBIOCHEM

# Supporting Information

CHEMBIOCHEM

# Supporting Information

for

## Allosteric Control of Ribozyme Catalysis by Using DNA Constraints

Elena Zelin and Scott K. Silverman*

**Table of Contents** page

General experimental considerations

DNA oligonucleotides and some RNA oligonucleotides were prepared by solid-phase synthesis at IDT (Coralville, IA). RNA transcripts were prepared with T7 RNA polymerase and a synthetic double-stranded DNA template that was prepared by annealing two DNA oligonucleotides.[1] The P4-P6 RNA was prepared by in vitro transcription with T7 RNA polymerase and a linearized plasmid template.[2] DNA and RNA oligonucleotides and transcripts were purified by denaturing PAGE as described previously.[3,4] The DNA constraint sequences shown in Figure 2b were chosen to avoid accidental complementarity to any part of the hammerhead ribozyme sequence. The upper complementary DNA strand was attached to A37e; the lower complementary strand was attached to A13e or A12s. The upper complementary DNA strand was also used as the free oligonucleotide used to disrupt the DNA constraint. After 5′-adenylation, a suitably 3′-modified version of the upper complementary DNA strand was used during the in vitro selection experiments as the R substrate (see below).

In vitro selection of deoxyribozymes that attach DNA to RNA

The selection experiments were performed essentially as described previously.[3,5] The 22 nucleotides shown in green in Figure S1a were random at the outset of the selection process. The L substrate was 5′-GGAUAAUACGACUCACUAUA-3′, where the branch-site adenosine is underlined. The R substrate was 5′-GGAAGAGATGGCGACr(GGA)-3′, where all nucleotides were DNA except the three 3′-terminal residues; this allowed ligation of the right-hand substrate to the deoxyribozyme strand with T4 RNA ligase. The R substrate (1 nmol) was 5′-adenylated using a template strand (5′-CCGTCGCCATC-TCTTCCTATAG-3′, 1.5 nmol) and T4 DNA ligase (Fermentas) as described,[6] with incubation conditions of 40 mM Tris, pH 7.8, 10 mM DTT, 10 mM $MgCl_2$, 6.5 mM ATP, and 20 U of T4 DNA ligase in 200 µL total volume at 25 °C for 1 h. The selection progression (i.e., ligation activity versus round number) is shown in Figure S1b. The incubation time during the key selection step was progressively decreased from 2 h to 10 min to 1 min as depicted. After round 9, individual deoxyribozymes were cloned and surveyed for ligation activity. The 9FQ4 deoxyribozyme (see sequence and secondary structure in Figure 1 and Figure S2 below) was chosen for further analysis based on its good ligation activity with model substrates (see below).

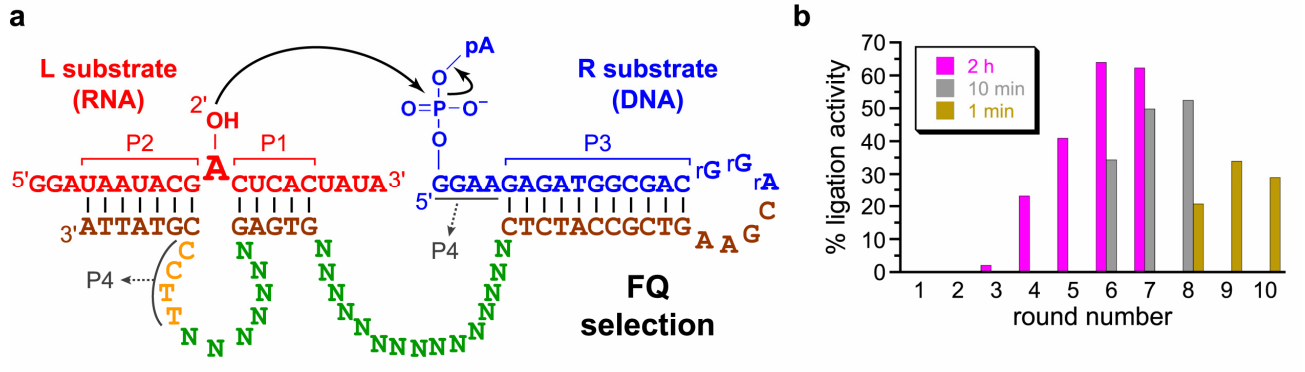


**Figure S1.** The FQ selection arrangement and activity progression. a) Selection arrangement. The 22 N nucleotides (green) were random at the outset of selection. b) Activity progression. Rounds 6 and 7 were each performed separately using two different incubation times as indicated. Round 8 was performed twice, both times using the 10 min product from round 7. Round 9 was performed using the 1 min product from round 8. Deoxyribozymes were cloned from round 9.

Kinetic assays of 9FQ4 deoxyribozyme ligation activities

For assays of 9FQ4 deoxyribozyme ligation activities using DNA from solid-phase synthesis, the general approach has been described previously.[3,5] The 5′-$^{32}$P-radiolabeled left-hand (L) substrate was the limiting reagent relative to the deoxyribozyme (E) and the right-hand (R) substrate. A 7 µL sample containing 1 pmol of L, 5 pmol of E, and 15 pmol of R was annealed in 5 mM Tris, pH 7.5, 15 mM NaCl, and 0.1 mM EDTA by heating at 95 °C for 3 min and cooling on ice for 5 min. The sample was adjusted to final concentrations of 50 mM CHES, pH 9.0, 150 mM NaCl and 2 mM KCl by addition of 2 µL of an appropriate stock solution. The ligation reaction was initiated by addition of 1 µL of 400 mM $MgCl_2$ (final $Mg^{2+}$ concentration of 40 mM), and the sample was incubated at 37 °C. Aliquots of 1–2 µL were removed at desired timepoints, quenched onto 8 µL of stop solution [80% formamide, 1× TBE, 50 mM EDTA, 0.025% bromophenol blue, 0.025% xylene cyanol], and analyzed by 20% PAGE. The yield versus time data were fit directly to first-order kinetics; i.e., yield = $Y\bullet(1 - e^{-kt})$, where $k = k_{obs}$ and $Y$ = final yield.

Testing the 9FQ4 deoxyribozyme with systematic model substrate sequences

The generality of 9FQ4 for its RNA and DNA substrates was assessed by using a systematic set of model substrates. The parent L RNA substrate was as given above. The parent R DNA substrate was as given above, except ending with 3′-terminal d(GG) rather than r(GGA). Systematic variants of L and R were created according to the following rules: transitions, A↔G and U↔C; transversions-1, A↔C and U↔G; transversions-2, A↔U and G↔C. The 5′-GGA of L was maintained in all cases to allow in vitro transcription. 5′-Adenylation of the variant DNA substrates proceeded well with the appropriately altered template strands except for the 5′-C DNA, for which the adenylation yield was greatly reduced. Nevertheless, sufficient adenylated product could be isolated. The binding arms of the deoxyribozyme were varied to maintain complete Watson-Crick complementarity with the RNA substrates.

The sequence of 9FQ4 along with the parent L and R substrates is shown in Figure S2a. Varying the only the branch-site nucleotide of L revealed that 9FQ4 greatly prefers a branch-site adenosine (Figure S2b). Branch-site C was used but with substantially lower efficiency, and branch-site G or U were not tolerated.

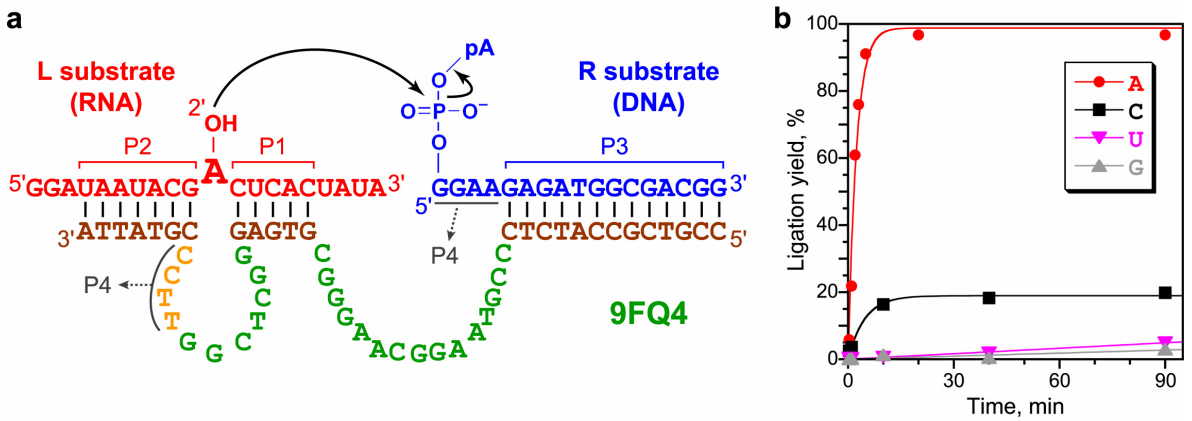


**Figure S2.** The 9FQ4 deoxyribozyme and testing of its ligation activity using L substrates with different branch-site nucleotides. a) Sequence and secondary structure of 9FQ4 complexed with the parent L and R substrate sequences. b) Ligation activity with the parent L substrate (branch-site A) and variant substrates with the other three branch-site nucleotides.

In all other assays of 9FQ4 with model substrates, the branch-site adenosine was unchanged. Systematic changes to the L RNA substrate except for the branch-site A suggested a useful degree of generality by 9FQ4 (Figure S3). The transversions-1 changes had little effect on rate or yield; the transversions-2 changes had a larger effect; and the transitions substantially suppressed ligation activity (Figure S3a). To narrow the source of the lower activity with transitions in L, these sequence changes were made only within the P1 or P2 regions (see Figure S2 above for designations of paired regions P1–P4). Transitions in P2 were tolerated well, whereas transitions in P1 were not tolerated well (Figure S3b). Attempts to dissect P1 by either varying only the first nucleotide adjacent to the branch-site or varying the other four nucleotides led in both cases to strong ligation activity (Figure S3c), suggesting that the specific sequence of L with transitions at all five positions of P1 is an unusually poor ligation substrate. Overall, we concluded that L can have a high level of change relative to the parent sequence and still be used as a substrate in a general way by the 9FQ4 deoxyribozyme.

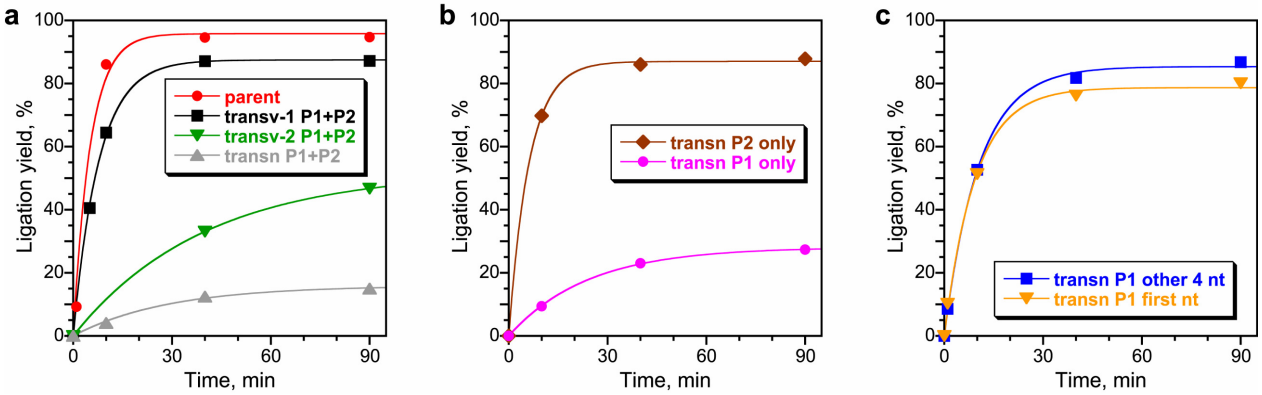


**Figure S3.** Testing of 9FQ4 activity using L substrates with systematic changes. a) Changes to all P1 and P2 nucleotides of L (see Figure S2 for designations of paired regions). b) Transitions in P1 or P2 alone. c) Transitions in P1 at only the first nucleotide adjacent to the branch site, or at the other four nucleotides.

Finally, systematic changes to the R DNA substrate were examined (Figure S4). When retaining the 5′-terminal G nucleotide, each of transitions, tranversions-1, and transversions-2 for all other nucleotides of R were tolerated well, with transitions tolerated somewhat less well than the other changes. Separately, when only the 5′-terminal G nucleotide was changed to A, C, or T, activity was progressively reduced, with 5′-A used well, 5′-C used with low activity, and 5′-T not tolerated.

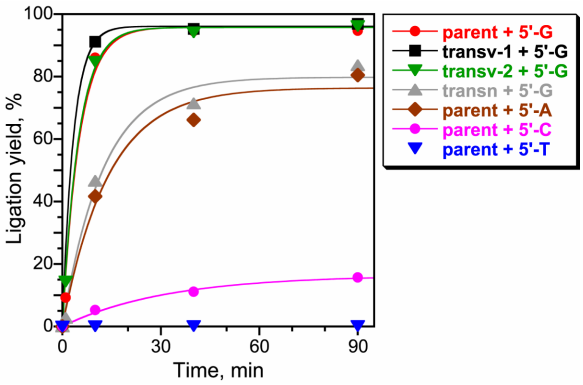


**Figure S4.** Testing of 9FQ4 activity using R substrates with systematic nucleotide changes. The 5′-nucleotide (originally G in the parent R substrate) was changed separately from all other nucleotides, which were either the parent sequence, transversions-1 (transv-1), transversions-2 (transv-2), or transitions (transn).

Testing 9FQ4 with the P4-P6 RNA as substrate

To explore the generality of 9FQ4 with an RNA substrate entirely unrelated to the sequence used in selection, we tested DNA attachment at ten adenosine nucleotides of the *Tetrahymena* group I intron P4-P6 domain.[7] Four of the ten sites were derivatized with DNA in at least 60% yield, and two other sites were modified in about 20% yield (Figure S5). The remaining four sites were derivatized poorly (<10% yield).

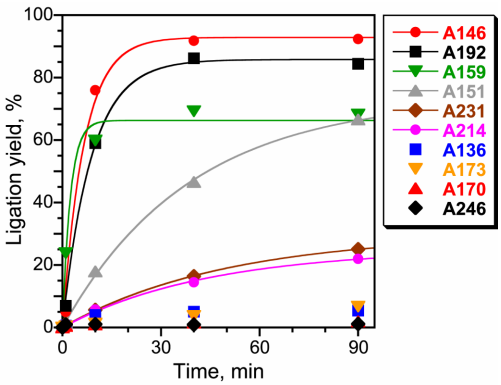


**Figure S5.** Testing of 9FQ4 activity using the P4-P6 RNA as substrate.

Testing 9FQ4 with the hammerhead ribozyme as substrate

To determine the useful DNA attachment sites by 9FQ4 on the hammerhead ribozyme, six enzyme-strand adenosines with solvent-exposed 2′-hydroxyl groups were chosen for testing. Three of the six sites were derivatized with DNA in at least 60% yield; one site was modified in about 20% yield, and the remaining two sites were derivatized poorly (<10% yield) (Figure S6a). Separately, site A12s on the substrate strand was also tested (Figure S6b). Under the standard 9FQ4 conditions (40 mM $Mg^{2+}$), the ligation yield was only about 10%. However, by increasing the $Mg^{2+}$ concentration to 120 mM, the yield was improved to nearly 30%, which was sufficient in practice to allow use of A12s as a DNA attachment site.

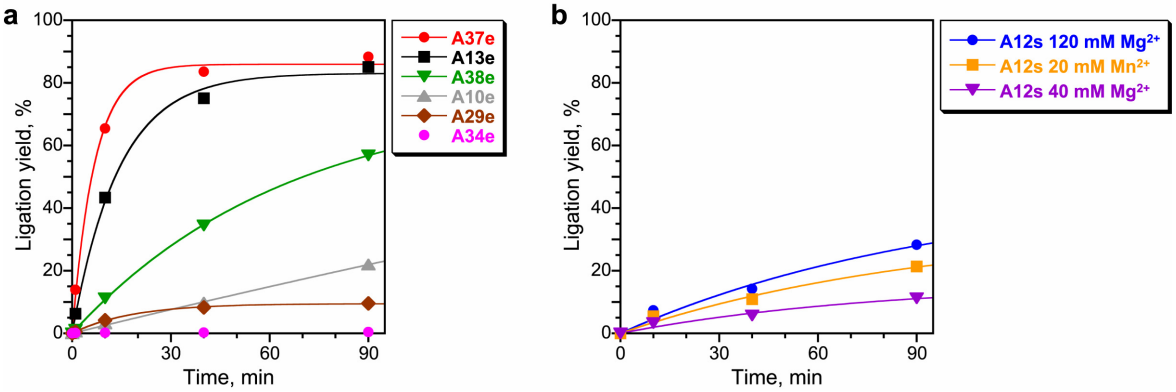


**Figure S6.** Testing of 9FQ4 activity using the hammerhead ribozyme RNA strands as substrates. a) Testing of six sites with the enzyme strand under the standard incubation conditions (40 mM $Mg^{2+}$). b) Testing of the A12s site within the substrate strand under various incubation conditions.

Computer modeling of the DNA-constrained hammerhead ribozyme

The computer modeling experiments were performed using an approach closely related to that described previously,[8] using MOE (Chemical Computing Group, Montreal), version 2004.3. It is important to note that the goal of this modeling was to provide a visual image that reasonably illustrates the DNA constraint strategy, rather than to provide a detailed molecular-scale model of the misfolded DNA-constrained ribozyme. To model the misfolded A13e-A37e ribozyme with the intact DNA duplex attached, the following three-step procedure was followed:

(1) The PDB structure of the hammerhead ribozyme (PDB id 2GOZ, chains A and B)[9] was imported and hydrogen atoms were added. Six fragments were defined, as follows. Fragment 1 = G1e–G14e + C7s–C20s; fragment 2 = C15e–A21e; fragment 3 = G22e–C36e; fragment 4 = G36e–A38e; fragment 5 = A39e–C43e + G1s–U5s; and fragment 6 = C6s. Fragments 1, 3, and 5 (corresponding to stems I, II, and III) were defined as rigid bodies, whereas fragments 2, 4, and 6 remained free.

(2) A 14-bp B-form DNA duplex was created from the two 15-nt strands of Figure 2b. The 14-bp region was defined as a rigid body, whereas the two 5′-terminal G nucleotides remained free. The DNA was manually positioned near the hammerhead ribozyme in approximately the orientation of Figure 2c, and the 5′-terminal G nucleotides of the DNA were connected to the 2′-hydroxyl groups of A13e and A37e.

(3) The structure was minimized using the stated rigid-body constraints to provide the final structure shown in Figure 2c.

An alternative colored version of key elements of Figure 2 is shown in Figure S7. The nucleotides of the ribozyme are colored as in the hammerhead ribozyme X-ray crystal structure manuscript.[9]

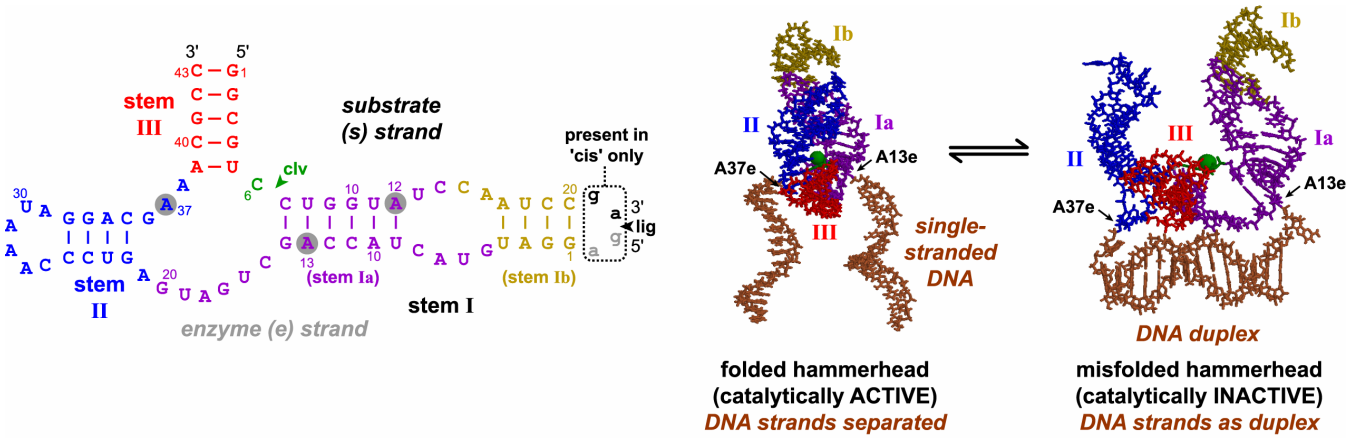


**Figure S7.** Alternative version of Figures 2a (left) and 2c (right), with nucleotides of the A13e-A37e ribozyme colored as previously published for the unmodified ribozyme.[9]

The A12s-A37e hammerhead ribozyme was also modeled (Figure S8). As described in the main text, the location of A12s at the remote end of stem Ia permits fraying of the A12s-U9e base pair along with stem Ib, so that the DNA duplex can form while maintaining the minimal hammerhead ribozyme core (the first 5 bp of stem Ia along with stems II and III). However, this may occur only for the 'trans' form of the ribozyme but not for the 'cis' form, because of the tetraloop capping stem Ib in the 'cis' form. Three states of the A12s-A37e ribozyme were modeled. Two of these structures (shown along the top of Figure S8) are directly analogous to those modeled for the A13e-A37e ribozyme. The third structure is unique to the 'trans' A12s-A37e ribozyme and demonstrates that the minimal hammerhead core may remain intact with the DNA duplex also present merely by separating stem Ib along with the final A-U base pair of stem Ia.

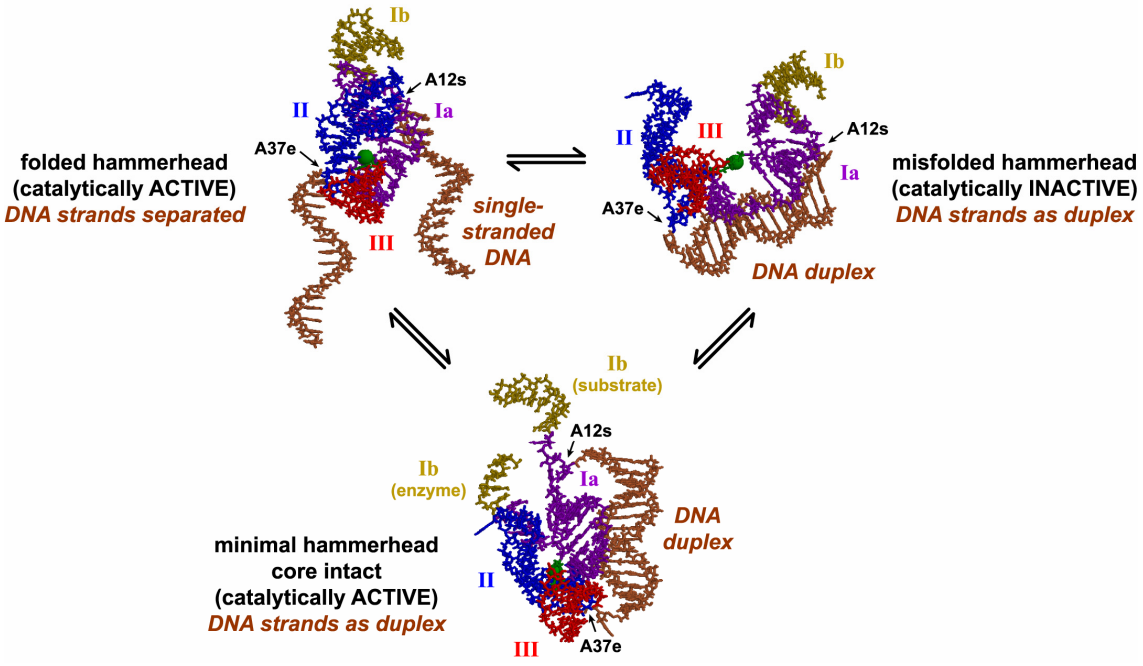


**Figure S8.** Modeling of the A12s-A37e hammerhead ribozyme. In the bottom structure, the minimal hammerhead core (i.e., the first 5 bp of stem Ia along with stems II and III) is in exactly the same conformation as found in the X-ray crystal structure (upper left structure), although the whole RNA-DNA complex has been rotated to highlight separation of stem Ib.

## Synthesis of hammerhead ribozyme substrate and enzyme strands

The ribozyme substrate strand was prepared by solid-phase synthesis at IDT. The ribozyme enzyme strand was prepared by in vitro transcription using a double-stranded DNA template and T7 RNA polymerase. For attachment of DNA strands, the L substrate (substrate or enzyme strand as appropriate) was the limiting reagent relative to the enzyme E (deoxyribozyme) and the R substrate (AppDNA). A typical synthesis used 400 pmol L, 440 pmol E, and 480 pmol R (for attachment of DNA to the enzyme strand) or 100 pmol L, 150 pmol E, and 200 pmol R (for attachment of DNA to the substrate strand). A 20 µL sample was annealed in 5 mM Tris, pH 7.5, 15 mM NaCl, and 0.1 mM EDTA by heating at 95 °C for 3 min and cooling on ice for 5 min. The sample was adjusted to final concentrations of 50 mM CHES, pH 9.0, 150 mM NaCl and 2 mM KCl by addition of 6 µL of an appropriate stock solution. The reaction was initiated by addition of 2.8 µL of water and 1.2 µL of 1 M $MgCl_2$ (final $Mg^{2+}$ concentration of 40 mM). The sample was incubated at 37 °C for 2 h, quenched onto 30 µL of stop solution, and purified by 12% PAGE. Typical yields were 50–60% for the first DNA attachment and 20–30% for the second DNA attachment (when performed).

For the 'trans' ribozyme assays, the enzyme strand was unradiolabeled, and the substrate strand was 5′-$^{32}$P-radiolabeled. To prepare the 'cis' ribozymes by ligation, ~15 pmol of 5′-$^{32}$P-radiolabeled enzyme strand was mixed with 25 pmol of DNA splint (5′-GCGTTTCGTCCTATTTGGGACTCATCAGCTGGTA-GTACATCCTCTCGGATTGGATACCAG-3′; the two DNA splint nucleotides across from the RNA ligation site are in boldface), and 30 pmol substrate strand in 9.6 μL of 5 mM Tris, pH 7.5, and 0.1 mM EDTA (no NaCl). The sample was annealed by heating at 95 °C for 3 min and cooling on ice for 5 min, then adjusted to 12 μL total volume containing 50 mM Tris, pH 8.0, 7.5 mM DTT, 10 mM $MgCl_2$, 1 mM ATP, and 12 U T4 RNA ligase (Fermentas). The sample was incubated at 37 °C for 4 h and purified by 12% PAGE. The typical yield of 'cis' ribozyme was >90%, with <10% hammerhead-catalyzed self-cleavage observed with the parent ribozyme or when noncomplementary DNA strands were attached; interestingly, no self-cleavage at all was observed (<0.5%) when the DNA strands were complementary. The products were extracted in Tris-EDTA buffer and precipitated using ethanol without adding NaCl. Although this resulted in only ~20% precipitation efficiency, the ribozyme was nearly free of autocatalytic cleavage product in the subsequent zero timepoints. In contrast, when NaCl was present during extraction and precipitation, appreciable (>50%) autocatalytic cleavage of the ribozyme was observed in the subsequent zero timepoints.

The 9FQ4 deoxyribozyme sequences were as follows. In each sequence, the enzyme loops are in boldface, and the P4 region is underlined. The DNA strand attached by the deoxyribozyme is given in parentheses. Strand 1 is the upper DNA sequence in Figure 1b; strand 2 is the lower sequence.

A37e (strand 1): 5′- GTCGCCATCTC**CCGTAAGGCAAGGGC**GCGTT**GGCTCGG**TTCCCGTCCTATTTGG -3′

A13e (strand 1): 5′- GTCGCCATCTC**CCGTAAGGCAAGGGC**TCAGC**GGCTCGG**TTCCGGTAGTACATCC -3′

A13e (strand 2): 5′- GAAGAGATGGC**CCGTAAGGCAAGGGC**TCAGC**GGCTCGG**GACCGGTAGTACATCC -3′

A12s (strand 1): 5′- GTCGCCATCTC**CCGTAAGGCAAGGGC**TTGGA**GGCTCGG**TTCCACCAGGACGCC -3′

A12s (strand 2): 5′- GAAGAGATGGC**CCGTAAGGCAAGGGC**TTGGA**GGCTCGG**GACCACCAGGACGCC -3′

Kinetic assays of hammerhead ribozyme activities

The 5′-$^{32}$P-radiolabeled substrate strand (S) was the limiting reagent relative to the enzyme strand (E). A 9 μL sample containing 0.4 pmol of S and 4 pmol of E was annealed in 50 mM Tris, pH 7.4, and 0.1 mM EDTA by heating at 95 °C for 2 min, 65 °C for 2 min, and 25 °C for 5 min. The reaction was initiated by addition of 1 μL of 50 mM $MgCl_2$ (final $Mg^{2+}$ concentration of 5 mM), and the sample was incubated at 25 °C (water bath). Aliquots of 1–2 μL were removed at desired timepoints, quenched onto 8 μL of stop solution, and stored on dry ice until analysis by 20% PAGE. Values of $k_{obs}$ were obtained by fitting the yield versus time data to first-order kinetics; i.e., yield = $Y\bullet(1 - e^{-kt})$, where $k = k_{obs}$ and $Y$ = final yield. When appropriate, a double-exponential equation was used instead: yield = $Y_1\bullet(1 - e^{-kt}) + Y_2\bullet(1 - e^{-k't})$. Others have noted that hammerhead ribozymes frequently display biphasic kinetics,[10] and biphasic kinetics were observed for the particular version of the hammerhead that was recently studied by X-ray crystallography[9] and also used as the basis of the present study. Tabulation of the kinetic data from Figures 3 and 5 is provided in Table S1.

| | Parent (–/–) | Compl/– | Compl/+ | Noncompl/– |
|---|---|---|---|---|
| **A13e-A37e 'cis'** (Figure 3a) | | | | |
| $k_{obs,1}$ ($min^{-1}$) | 10.3 ± 0.8 | 4.3 ± 0.8 | 9.8 ± 0.8 | 14.5 ± 2.9 |
| $\%_1$ | 74 ± 2 | 19 ± 1 | 61 ± 1 | 58 ± 1 |
| $k_{obs,2}$ ($min^{-1}$) | 0.65 ± 0.16 | 0.12 ± 0.03 | 0.10 ± 0.01 | 0.13 ± 0.02 |
| $\%_2$ | 10 ± 2 | 14 ± 1 | 20 ± 1 | 21 ± 1 |
| sum of % | 84 | 33 | 81 | 79 |
| **A13e-A37e 'trans'** (Figure 3b) | | | | |
| $k_{obs,1}$ ($min^{-1}$) | 8.4 ± 0.5 | 0.06 ± 0.01 | 3.1 ± 0.3 | 0.35 ± 0.06 |
| $\%_1$ | 76 ± 1 | 19 ± 2 | 69 ± 3 | 51 ± 9 |
| $k_{obs,2}$ ($min^{-1}$) | 0.22 ± 0.04 | n/a | 0.09 ± 0.04 | 0.05 ± 0.03 |
| $\%_2$ | 12 ± 1 | n/a | 18 ± 3 | 37 ± 5 |
| sum of % | 88 | 19 | 87 | 88 |
| **A12s-A37e 'cis'** (Figure 5a) | | | | |
| $k_{obs,1}$ ($min^{-1}$) | 14.4 ± 2.4 | 0.40 ± 0.08 | 10.4 ± 1.4 | 2.7 ± 0.2 |
| $\%_1$ | 73 ± 1 | 19 ± 1 | 58 ± 1 | 53 ± 2 |
| $k_{obs,2}$ ($min^{-1}$) | 0.18 ± 0.03 | n/a | 0.17 ± 0.03 | 0.04 ± 0.03 |
| $\%_2$ | 14 ± 1 | n/a | 20 ± 1 | 22 ± 5 |
| sum of % | 87 | 19 | 78 | 75 |
| **A12s-A37e 'trans'** (Figure 5b) | | | | |
| $k_{obs,1}$ ($min^{-1}$) | 7.7 ± 0.9 | 0.31 ± 0.07 | 1.0 ± 0.1 | 0.67 ± 0.09 |
| $\%_1$ | 59 ± 2 | 26 ± 5 | 31 ± 2 | 61 ± 6 |
| $k_{obs,2}$ ($min^{-1}$) | 0.23 ± 0.03 | <0.02 | 0.03 ± 0.01 | 0.04 ± 0.03 |
| $\%_2$ | 30 ± 2 | >14 | 58 ± 11 | 30 ± 9 |
| sum of % | 89 | >40 | 89 | 91 |

Table S1. Tabulation of kinetic parameters from the data in Figures 3 and 5. The four columns represent lanes 1–4 for each figure panel. The $k_{obs}$ values and % cleavage values for both components of the biphasic fits are shown, as is the sum of the two % values for reference. Errors are standard deviations from the curve fits. Entries of "n/a" ("not applicable") for the second component indicate that a monophasic curve fit was sufficient.

Modulation of the DNA constraint effect using DNase I

The procedure was performed by the approach described previously,[11] using the A13e-A37e DNA-constrained hammerhead ribozyme. The 5′-$^{32}$P-radiolabeled substrate strand (0.2 pmol) and the enzyme strand (2 pmol, with attached DNA strands as appropriate) were treated according to the kinetic assay procedure described in the previous section, except that 1 mM NaCl, 10 mM $MgCl_2$, 1 mM $CaCl_2$, and 20 U of RNase inhibitor (Roche) were included in each 10 µL sample. In the sample containing DNase, 1 U of RQ1 DNase (Promega) was added at the same time as the metal ions. The kinetic data were acquired at 37 °C, which is the optimal incubation temperature for DNase I (note that the other hammerhead ribozyme kinetics in this manuscript were all obtained at 25 °C). The results (Figure S9) revealed that the reduced activity due to the DNA constraint was increased substantially upon addition of DNase. Because DNase likely cannot remove every DNA nucleotide attached to the RNA (but enough DNA nucleotides are removed to destroy the DNA constraint), the activity after DNase addition was expected to resemble the "noncomplementary strands" ribozyme (i.e., to have modestly suppressed reaction rate), which was observed. Furthermore, the observed cleavage activity may be rate-limited not by the hammerhead ribozyme cleavage reaction but by the action of DNase, for which the activity has not been fully investigated in the context of cleaving DNA strands that are covalently attached to RNA.

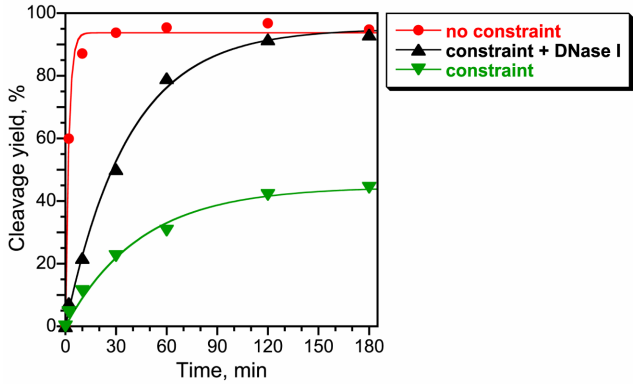


**Figure S9.** Modulating the DNA constraint effect on hammerhead ribozyme activity by adding DNase I to destroy the constraint.

Probing hammerhead ribozyme secondary structure with RNase T2

The RNase T2 probing experiments of Figure 4, which examine the presence of stems I and III, were performed using 5′-$^{32}$P-radiolabeled substrate strand (S) and unradiolabeled enzyme strand (E). A 9 µL sample containing 1 pmol of S and 10 pmol of E was annealed in 50 mM Tris, pH 7.4, and 1 mM EDTA by heating at 95 °C for 2 min, 65 °C for 2 min, and 25 °C for 5 min. To the sample was added 1 µL of 100 mM $MgCl_2$ (final net $Mg^{2+}$ concentration of 9 mM), and the sample was incubated for 20 min at 25 °C. Then, 0.5 µL of RNase T2 (0.01 U/µL, Invitrogen) or 1 µL of RNase T1 (2 U/µL, Ambion, to calibrate the partial alkaline hydrolysis ladder) was added, and the sample was incubated for 10 min at 25 °C. The final concentration of RNase T2 was 0.0005 U/µL; the final concentration of RNase T1 was 0.2 U/µL. The partial alkaline hydrolysis sample was prepared by incubating S in 50 mM $NaHCO_3$, pH 9.2, and 0.1 mM EDTA for 2 min at 90 °C. The samples were analyzed by 20% PAGE.

The RNase T2 experiment to examine the presence of stem II is shown in Figure S10. The procedure was the same as above, except 1 pmol of radiolabeled E and 10 pmol of unradiolabeled S were used.

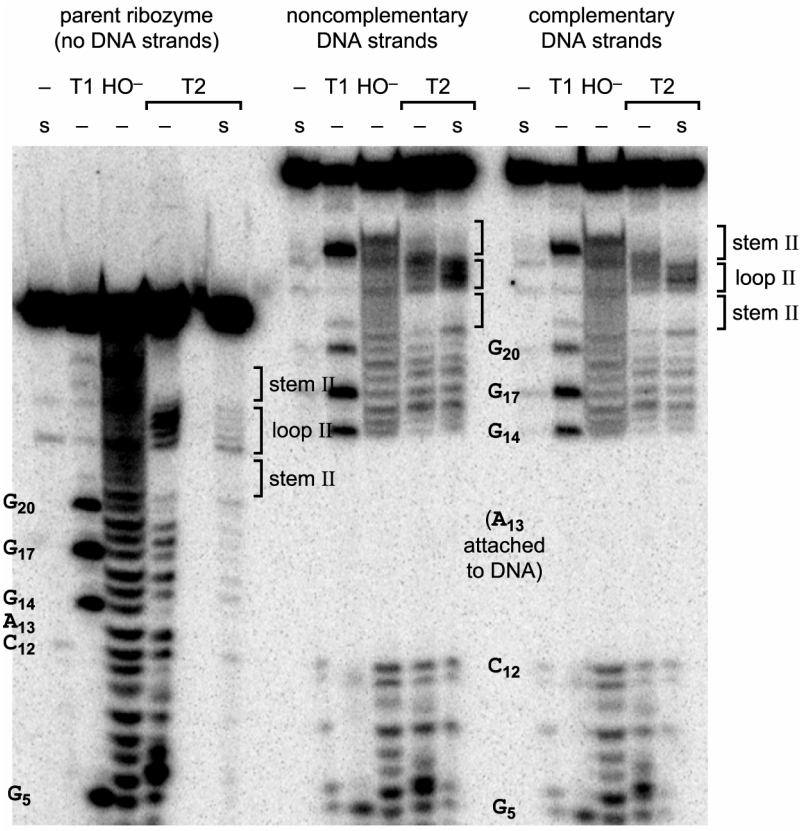


**Figure S10.** RNase T2 probing using 5′-$^{32}$P-radiolabeled enzyme strand to provide support for the presence of stem II in the A13e-A37e DNA-constrained hammerhead ribozyme. Protections of the stem II nucleotides relative to the loop II nucleotides are unambiguous (bracketed regions of gel image).

## References for Supporting Information

[1] J. F. Milligan, D. R. Groebe, G. W. Witherell, O. C. Uhlenbeck, *Nucleic Acids Res.* **1987**, *15*, 8783-8798.
[2] a) S. K. Silverman, T. R. Cech, *Biochemistry* **1999**, *38*, 8691-8702; b) S. K. Silverman, T. R. Cech, *Biochemistry* **1999**, *38*, 14224-14237.
[3] A. Flynn-Charlebois, Y. Wang, T. K. Prior, I. Rashid, K. A. Hoadley, R. L. Coppins, A. C. Wolf, S. K. Silverman, *J. Am. Chem. Soc.* **2003**, *125*, 2444-2454.
[4] Y. Wang, S. K. Silverman, *Biochemistry* **2003**, *42*, 15252-15263.
[5] E. Zelin, Y. Wang, S. K. Silverman, *Biochemistry* **2006**, *45*, 2767-2771.
[6] W. Chiuman, Y. Li, *Bioorg. Chem.* **2002**, *30*, 332-349.
[7] a) F. L. Murphy, T. R. Cech, *Biochemistry* **1993**, *32*, 5291-5300; b) J. H. Cate, A. R. Gooding, E. Podell, K. Zhou, B. L. Golden, C. E. Kundrot, T. R. Cech, J. A. Doudna, *Science* **1996**, *273*, 1678-1685.
[8] C. V. Miduturu, S. K. Silverman, *J. Am. Chem. Soc.* **2005**, *127*, 10144-10145.
[9] M. Martick, W. G. Scott, *Cell* **2006**, *126*, 309-320.
[10] T. K. Stage-Zimmermann, O. C. Uhlenbeck, *RNA* **1998**, *4*, 875-889.
[11] C. V. Miduturu, S. K. Silverman, *Angew. Chem.* **2006**, *45*, 1918-1921; *Angew. Chem. Int. Ed.* **2006**, *45*, 1918-1921.